

Supplementary Information

Selective hydrogenation of furfural using a membrane reactor

Roxanna S. Delima,^{1,2} Mia D. Stankovic,³ Benjamin P. MacLeod,^{2,3} Arthur G. Fink,³ Michael B. Rooney,³ Aoxue Huang,³ Ryan P. Jansonius,³ David J. Dvorak,² Curtis P. Berlinguette^{1,2,3,4*}

¹Department of Chemical and Biological Engineering, The University of British Columbia, 2360 East Mall, Vancouver, British Columbia, V6Y 1Z3, Canada.

²Stewart Blusson Quantum Matter Institute, The University of British Columbia, 2355 East Mall, Vancouver, British Columbia, V6T 1Z4, Canada.

³Department of Chemistry, The University of British Columbia, 2036 Main Mall, Vancouver, British Columbia, V6T 1Z1, Canada.

⁴Canadian Institute for Advanced Research (CIFAR), MaRS Centre, West Tower, 661 University Avenue, Toronto, Ontario, M5G 1M1, Canada

*Corresponding author: Curtis P. Berlinguette (cberling@chem.ubc.ca)

Table of Contents

MultiThor Construction and Assembly	2
Supplementary Experimental Methods	4
Additional Membrane Preparation and Characterization	4
Sputter-Deposition Procedure	4
Electrochemical Surface Area (ECSA) Measurements	5
X-ray Fluorescence (XRF) Spectroscopy	6
Scanning Electron Microscopy (SEM)	8
Furfural Proof-of-Concept Reaction in an H-cell	8
MultiThor Control Experiments	9
Hydrogen Distribution	9
Hydrogenation Distribution	10
Product Quantification by Gas Chromatography–Mass Spectrometry	12
Influence of Current and Charge Passed on Furfural Hydrogenation Rates	14
Influence of Sputter-Deposited Catalyst Thickness on Reactivity	15
Furfural Hydrogenation Without an Electrochemical Bias	16
Supplementary References	18

MultiThor Construction and Assembly

The custom components of MultiThor were designed in Solidworks Computer Aided Design (CAD) software, and manufactured in-house (Fig. S1). The hydrogenation compartment was machined from a block of polyetheretherketone (PEEK), and the electrochemical compartment was printed with a stereolithography (SLA) 3D Form 3 printer (made by Formlabs). The 3D print enabled the inclusion of complex internal features and flow channels that otherwise would not be possible to manufacture from conventional machining techniques. The electrochemical compartment contained an inlet flow channel that split into six individual tubes to direct electrolyte vertically towards each of the six wells (to aid H₂ bubble dispersion). The electrochemical compartment also contained 2 mm diameter horizontal flow channels that directed bubbles away from the Pd surface towards the electrolyte outlet (Fig. S2). The electrochemical compartment was printed from Formlabs proprietary clear V4 resin. The resin was chosen for its transparent optical properties, chemical resistance to the electrolyte, and watertight surface finish. Post-processing (e.g., wet sanding, thread chasing, and hole reaming) was required to fit and finish the compartment after printing and curing. Quick-turn polycarbonate couplings (1/4-28") were used to attach tubing from the electrochemical compartment to the pump and reservoir. Female threads were printed into the cell to fit these couplings (metal threaded inserts were not used because they are incompatible with the electrochemical process). The catalyst-coated Pd membrane was sealed between the hydrogenation and electrochemical compartments by custom laser-cut 1/16" thick fluorosilicone gaskets. Two 3/8" thick stainless steel plates sandwiched the two compartments, and eight 4 mm diameter bolts provided the clamping force to seal the internal gaskets (these bolts thread into the bottom plate). Two internal 5 mm diameter stainless steel locating pins were pressed into the bottom plate; these allowed precise assembly and disassembly of the cell. The Pt anode was shielded by a teflon body (1/4"

outer diameter), which was press-fitted into one side of the electrochemical compartment to provide a water-tight seal (a viton o-ring and bracket was used to provide an additional seal against the teflon body of the electrode). A $\frac{3}{8}$ " thick laser-cut acrylic panel was bolted to the bottom face of the electrochemical compartment to provide a viewing window (sealed with a viton o-ring). The viewing window enabled visual monitoring of H₂ bubble dispersion during experiments.

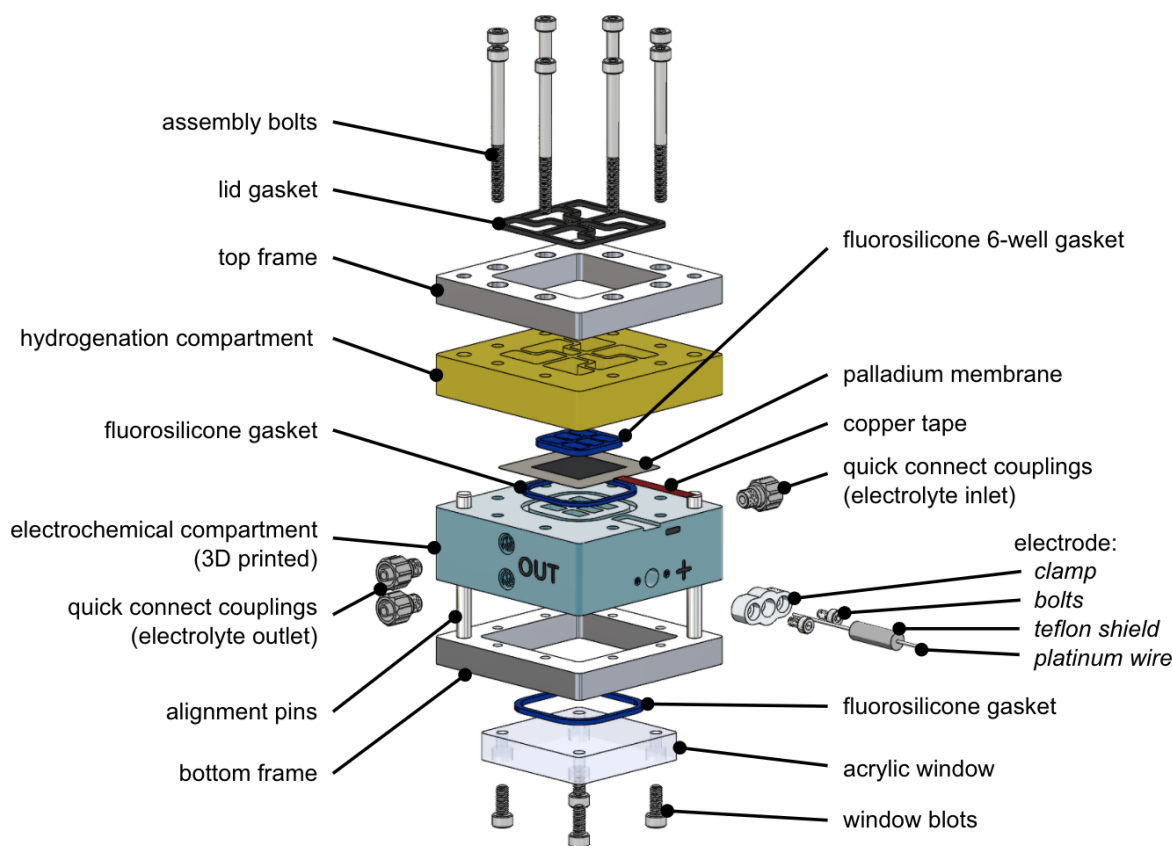


Figure S1: Exploded view of MultiThor assembly.

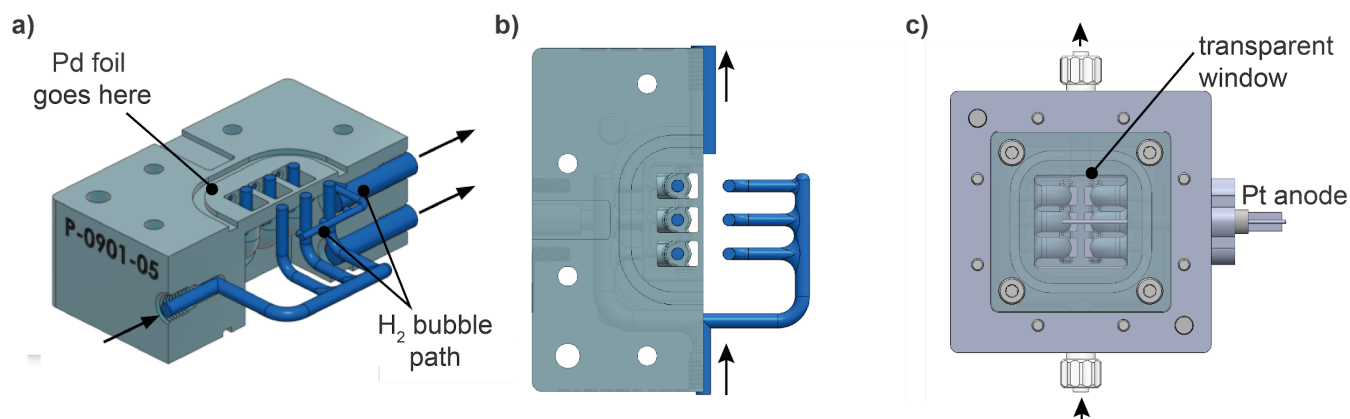


Figure S2: Electrochemical compartment of MultiThor with electrolyte flow channels: (a) side view; (b) top view; and (c) bottom view. Electrolyte flow to the Pd foil is highlighted in blue. Arrows indicate direction of electrolyte flow into and out of MultiThor (flow rate of 250 mL min⁻¹). The flow channels were designed to remove excess H₂ bubbles formed during water electrolysis at the Pd foil surface on the electrochemical side of the reactor.

Supplementary Experimental Methods

Additional Membrane Preparation and Characterization

Sputter-Deposition Procedure

An additional layer of catalyst was sputter-deposited on the Pd/Pd membranes based on previously reported procedures.¹ A Leica EM MED020 coating system was used to sputter-deposit Pt, Ir, Cu, Ag, and Au and a Univex 250 RF magnetron sputter system with an Onyx-2 IC Mag II cathode was used to deposit Ni. Pd/Pd membranes were placed at a working distance of 6 cm and the chamber was evacuated to a base pressure of 1.5×10^{-4} mbar (and 12 cm, 5×10^{-6} mbar, respectively for Ni). After the base pressure was reached, Ar gas was directed into the chamber at a continuous flow rate to maintain a pressure of 1×10^{-2} mbar, the plasma was ignited, and voltage was adjusted to maintain a constant current of 80 mA for Ir, and 30 mA for Au, Ag, Cu, and Pt. The RF power was held at 100 W for Ni. A 30 s pre-sputter (1 min for Ag and 6 min for Ni) was followed by the opening the target shutter and

sputter-deposition of 10 to 50 nm of metal catalyst onto the Pd/Pd membrane. The sputter rates were 0.2 nm/s (Pt, Cu, and Ni) and 0.3 nm/s (Ir, Au, and Ag), as determined by *in situ* quartz crystal microbalance. Once deposition was complete, the shutter was closed, chamber vented, and catalyst coated Pd membranes were removed from the deposition plate.

Electrochemical Surface Area (ECSA) Measurements

ECSA measurements of three different Ir/Pd/Pd membranes (geometric surface area of 4 cm²) with 0, 20, and 50 nm of sputter-deposited Ir catalyst were performed in the one-compartment electrochemical cell. The compartment was filled with 15 mL of 0.15 M tetrabutylammonium hexafluorophosphate (TBA-PF₆) in CH₃CN₄. A leak-free Ag/AgCl reference electrode using a leakless junction (eDAQ ET072) was used for ECSA measurements. The electrode was rinsed with Milli-Q water prior to use and referenced vs. 4.0 M KCl glass-body Ag/AgCl master reference electrode (Fisher Scientific 13-620-53) by measuring the open circuit potential between both electrodes in a saturated KCl solution. The master electrode was stored in a KCl solution when not in use. A 1 cm² Pt mesh counter electrode was used and cyclic voltammograms were performed at various scan rates (10 to 100 mV s⁻¹) with a potential range of 0.05 to 0.25 V versus Ag/AgCl. Current versus scan rates were plotted at 0.49, 0.47, and 0.52 V versus Ag/AgCl (the open circuit voltages) for 0, 20, and 50 nm, respectively. The slope of the plot was used to measure double-layer capacitance (Fig. S3).

We have previously reported double-layer capacitance values for Pd/Pd membranes with no additional sputter-deposited catalysts (i.e., 0 nm) of ~8.0 mF cm⁻² using the same deposition method and parameters and ECSA measurement procedure.^{2,3} ECSA measurements performed on 0 nm catalyst on Pd/Pd membranes in this study demonstrated a double-layer capacitance of 6.6 mF cm⁻² (Fig. S3). These collective results indicate that the electrodeposited Pd catalyst on Pd membranes can vary in surface area

by approximately $\pm 1.7 \text{ mF cm}^{-2}$. The double-layer capacitance values for 0, 20, and 50 nm thick sputter-deposited catalysts on the Pd/Pd membranes were within an error of $\pm 0.6 \text{ mF cm}^{-2}$. These findings suggest that the difference in double-layer capacitance values can be attributed to the underlying high surface area Pd catalyst, with little to no change in surface area from the sputter-deposited catalysts. ECSA was calculated for Pd/Pd membranes by dividing double-layer capacitance by specific capacitance of Pd. Specific capacitance was calculated using bare Pd foil because it embodies an atomically smooth planar Pd surface.^{4,5} ECSA calculations indicated that the Pd/Pd membranes have a chemical surface area that is 218 ± 23 times larger than bare Pd foil.

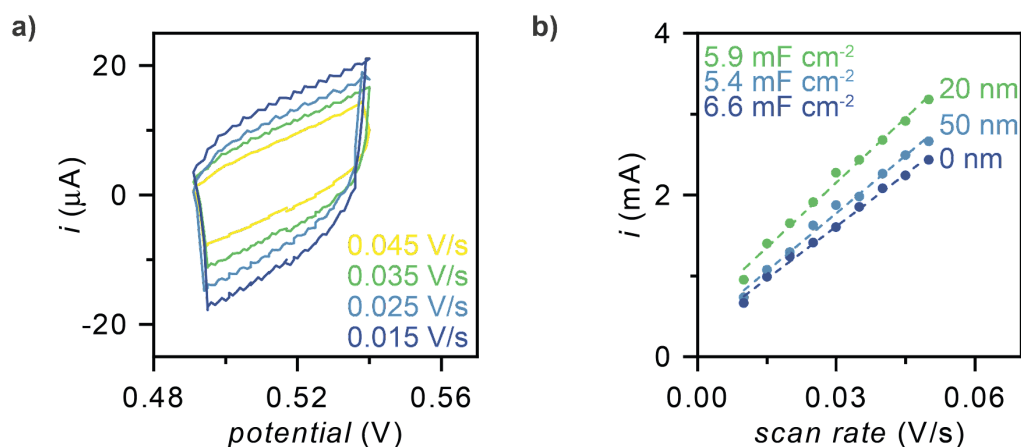


Figure S3: Electrocatalytic surface area (ECSA) measurements for different thicknesses of Ir sputter-deposited on Pd/Pd membranes. (a) CV scans near the open circuit potential (OCP; 0.52 V) for Ir catalyst (50 nm). (b) Double-layer capacitance measurements of Ir/Pd/Pd membrane (0, 20, and 50 nm Ir thicknesses). The open circuit voltages were 0.49, 0.47, and 0.52 V for 0, 20, and 50 nm, respectively. Double-layer capacitance values were calculated based on measured data. The dotted lines represent lines of best fit for the 9 data points. The geometric surface area of all cathodes was 4 cm^2 .

X-ray Fluorescence (XRF) Spectroscopy

Hyperspectral XRF images of the catalyst coated Pd membranes were taken using a Bruker M4 TORNADO XRF microscope. The XRF microscope has a Rh X-ray source operated at 50 kV/600 μA /30 W and polycapillary X-ray optics yielding a 25- μm spot size on the sample. The instrument

employs twin 30 mm² silicon SSD detectors and achieves an energy resolution of 10 eV. Hyperspectral images were taken over a 641×231 mm² area at a resolution of 750×270 pixels. The instrument generates a peak at exactly zero energy which is used for energy calibration. Each point measurement was integrated for 50 ms. The spectral energy is binned at 10 eV. Spectra was acquired from 0 to 40 keV and integrated over the following ranges: Pd: 2.632 to 2.892 keV (K α); Ni: 7.358 to 7.588 keV (K α); Au: 9.579 to 9.830 (L α); Cu: 7.925 to 8.162 keV (K α); Ir: 9.106 to 9.232 keV (L α); Pt: 9.374 to 9.498 keV (L α). Each element was visualized with a colour scale extending to the data bounds, with the exception of the following elements where the maximum was set manually for an improved visualization: Ni: 2.5×10⁵ cps; Cu: 2×10⁶ cps; Au: 5×10⁵ cps. XRF images of Ag were not obtained because the L α Ag lines were obscured by the higher intensity L α Pd lines.

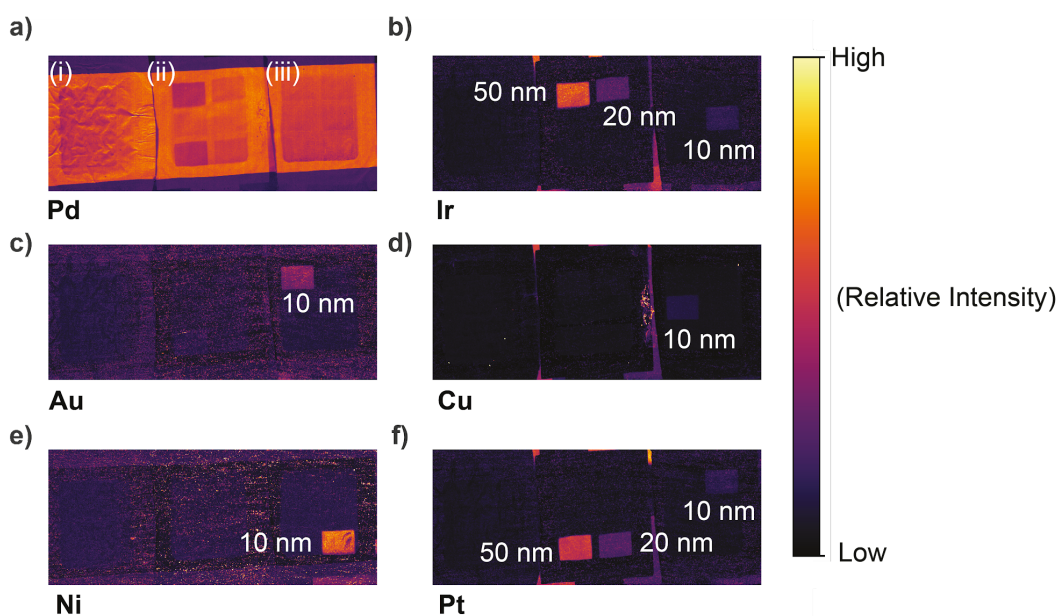


Figure S4: X-ray fluorescence (XRF) images for three prepared Pd foils. (a)–(f) XRF images of: (i) electrodeposited Pd catalyst on Pd foil membrane (Pd/Pd membrane); (ii) Pd/Pd membrane with 20 and 50 nm of sputtered catalysts (Ir (b), Pt (f)); and (iii) Pd/Pd membrane with 10 nm of sputtered catalysts (Ir (b), Au (c), Cu (d), Ni (e), Pt (f), Ag (now shown)).

Scanning Electron Microscopy (SEM)

SEM images of 10, 20, and 50 nm of sputter-deposited Ir on Pd/Pd membranes (Fig. 5c) were taken with an FEI Helios NanoLab 650 dual beam SEM at 1 kV and 50 pA using a through-lens detector in secondary electron mode. A horizontal field width (HFW) of 5.97 mm was exposed in all cases.

Furfural Proof-of-Concept Reaction in an H-cell

Initial proof-of-concept hydrogenation of furfural was performed in a two-compartment H-cell reactor consisting of an electrochemical and hydrogenation compartment (Fig. S5a). These compartments were filled with 30 mL of 1 M H₂SO₄ and 0.25 M furfural dissolved in *n*-BuOH, respectively. A current of 45 mA was applied across the Pd foil cathode (geometric surface area of 1.22 cm² on both sides) and Pt anode. A sample taken after 12 h of reaction showed that ~30% furfural was hydrogenated to form FA, THFA, and >6 products with higher retention time.

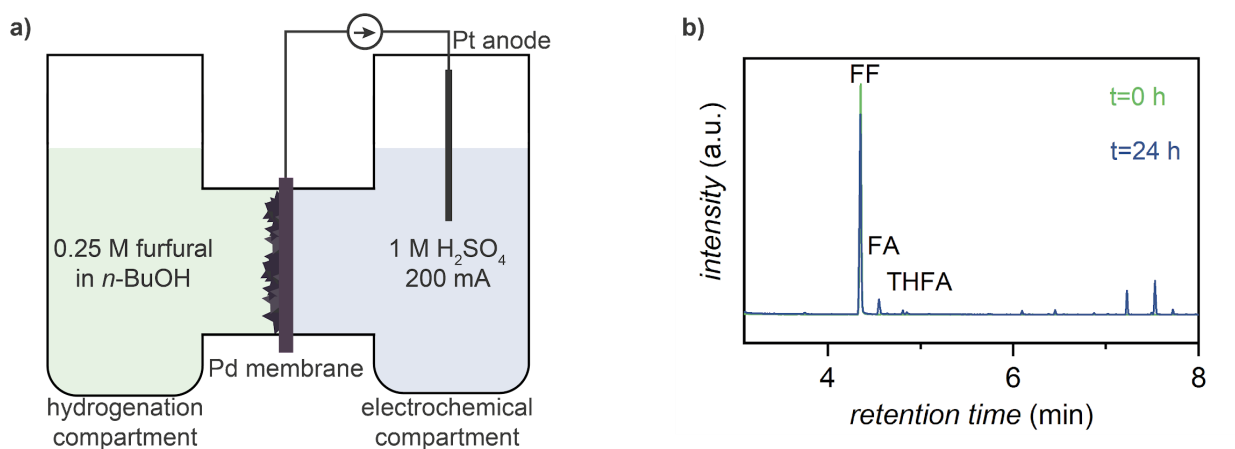


Figure S5: Proof-of-concept furfural hydrogenation experiment in an H-cell. (a) Schematic diagram of the H-cell electrocatalytic palladium membrane reactor architecture. (b) Gas chromatography–mass spectrometry measurements of furfural (FF) hydrogenation to furfuryl alcohol (FA), tetrahydrofurfuryl alcohol (THFA), and other products. A current of 45 mA was applied for 12 h. The Pd foil membrane had a geometric surface area of 1.22 cm².

MultiThor Control Experiments

Table S1: A qualitative comparison of the MultiThor and H-cell electrocatalytic palladium membrane reactor architectures based on the exposure of the hydrogenation solution to the catalyst surface.

	H-cell	MultiThor
Geometric surface area (SA)	1.22 cm ²	0.43 cm ²
Hydrogenation compartment volume (V)	30 mL	1 mL
Ratio of surface area:volume (SA/V)	~0.04 cm ² mL ⁻¹	0.43 cm ² mL ⁻¹
SA/V for MultiThor:H-cell	–	~10
Initial furfural consumption rate	6.3 μmol h ⁻¹	64.8 μmol h ⁻¹

Hydrogen Distribution

We tested hydrogen evolution on both sides of the Pd membrane to confirm that hydrogen permeation was evenly distributed across the six wells of the reactor (Fig. S6a). For these tests, a Pd/Pd membrane was placed in MultiThor, the hydrogenation wells were filled with 1 mL of *n*-BuOH, and a current of 75, 150, 225, or 300 mA was applied for 1 h. An atm-MS was used to measure the relative amount of H₂ evolved in each hydrogenation well and the electrochemical compartment, with hydrogen flux being defined as the amount of H₂ evolved in each well per unit time (Fig. S6b). Experiments performed with applied currents of 75, 150, and 225 mA showed hydrogen fluxes within error for each applied current (0.23±0.01 mmol h⁻¹, 0.45±0.03 mmol h⁻¹, and 0.65±0.03 mmol h⁻¹, respectively). An applied current of 300 mA resulted in hydrogen fluxes ranging from 0.62 mmol h⁻¹ to 0.78 mmol h⁻¹ for wells 1–6. Although the hydrogen flux between wells fluctuated at 300 mA, fluxes within each well were still consistent (e.g., well 1 consistently showed a hydrogen flux of ~0.76 mmol h⁻¹ for 3 different foils). We also found that >10% of H₂ evolved in the electrochemical compartment at 300 mA, compared to <10% H₂ at ≤225 mA. One possible explanation for these results is that at 300 mA, H₂

bubble formation blocked hydrogen from permeating, particularly the middle wells (well 3 and 4; Fig. S6c). Based on this finding, applied currents of ≤ 225 mA were used for all hydrogenation experiments.

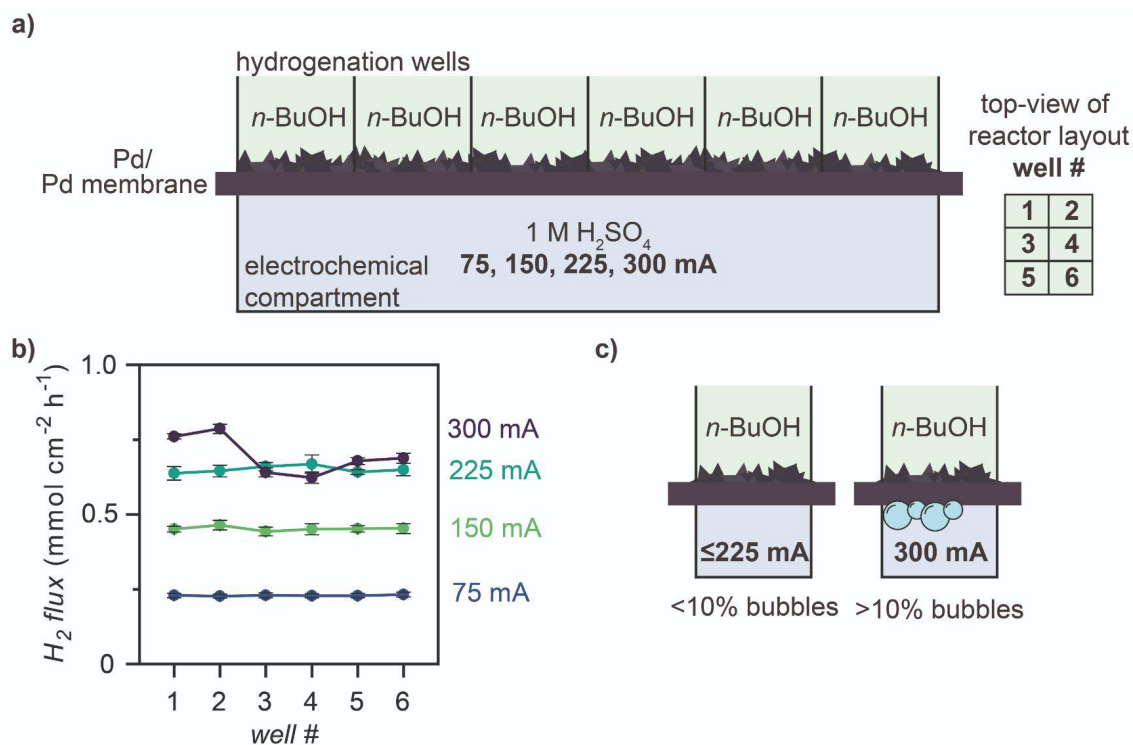


Figure S6: Hydrogen flux measurements for the 6 wells of MultiThor at different applied currents. (a) Schematic diagram of reactor setup with inset showing well position labelled 1–6. (b) Hydrogen (H_2) flux for each well at 75, 150, 225, and 300 mA. (c) Schematic diagram showing >10% H_2 bubble build up at an applied current of 300 mA compared to <10% bubble build up at ≤ 225 mA. H_2 flux was determined by atmospheric–mass spectrometer measurements of the ratio of H_2 evolved on the hydrogenation:electrochemical compartments.

Hydrogenation Distribution

The hydrogenation of 0.25 M furfural in *n*-BuOH was used as a proof-of-concept reaction to confirm that the rate of reaction was similar between wells (Fig. S6). A Pd/Pd membrane was placed in the MultiThor and a current of 150 mA was applied for 2 h. Reaction progress was monitored using gas chromatography–mass spectrometry (GC–MS) by taking 30- μ L aliquots from each well after 0, 0.5, 1, and 2 h. GC–MS measurements showed that hydrogenation proceeded at similar rates (<3% difference

in furfural consumption) for wells 1–6, respectively (Fig. S7). These data confirmed that hydrogenation occurs at similar rates across the six wells under the stated reaction conditions.

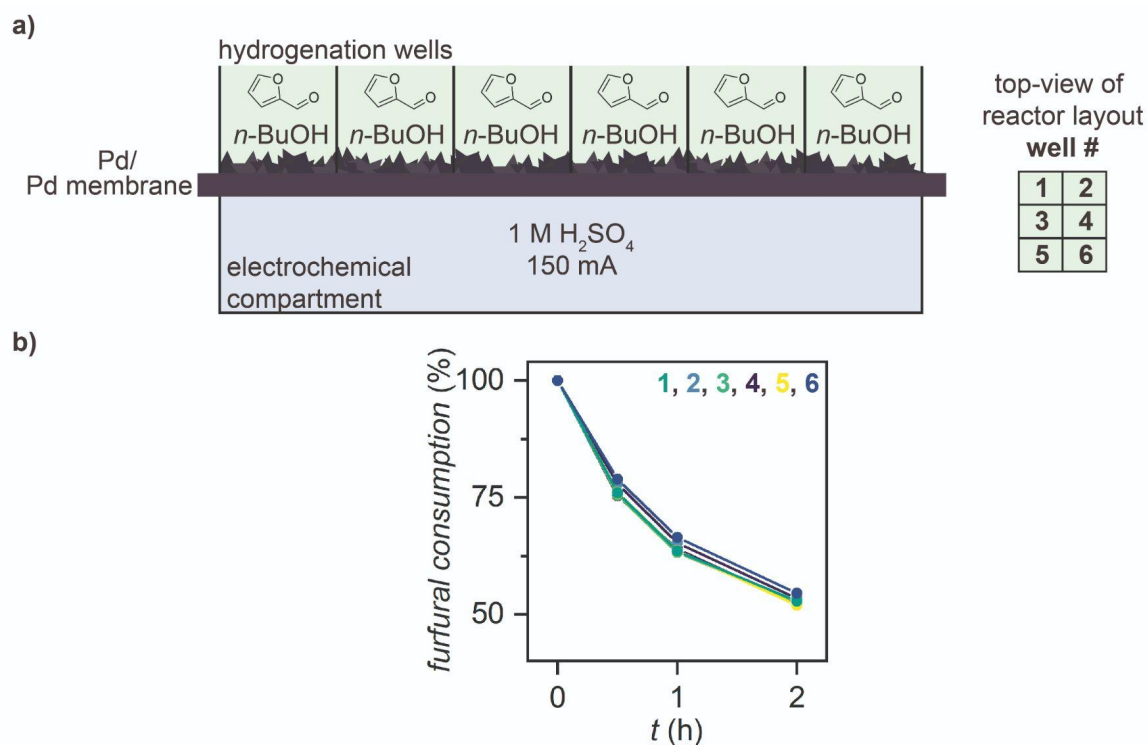


Figure S7: Furfural hydrogenation in the 6 wells of MultiThor. (a) Schematic diagram of reactor setup and (b) initial furfural consumption for 2 h of reaction in each well.

Product Quantification by Gas Chromatography–Mass Spectrometry

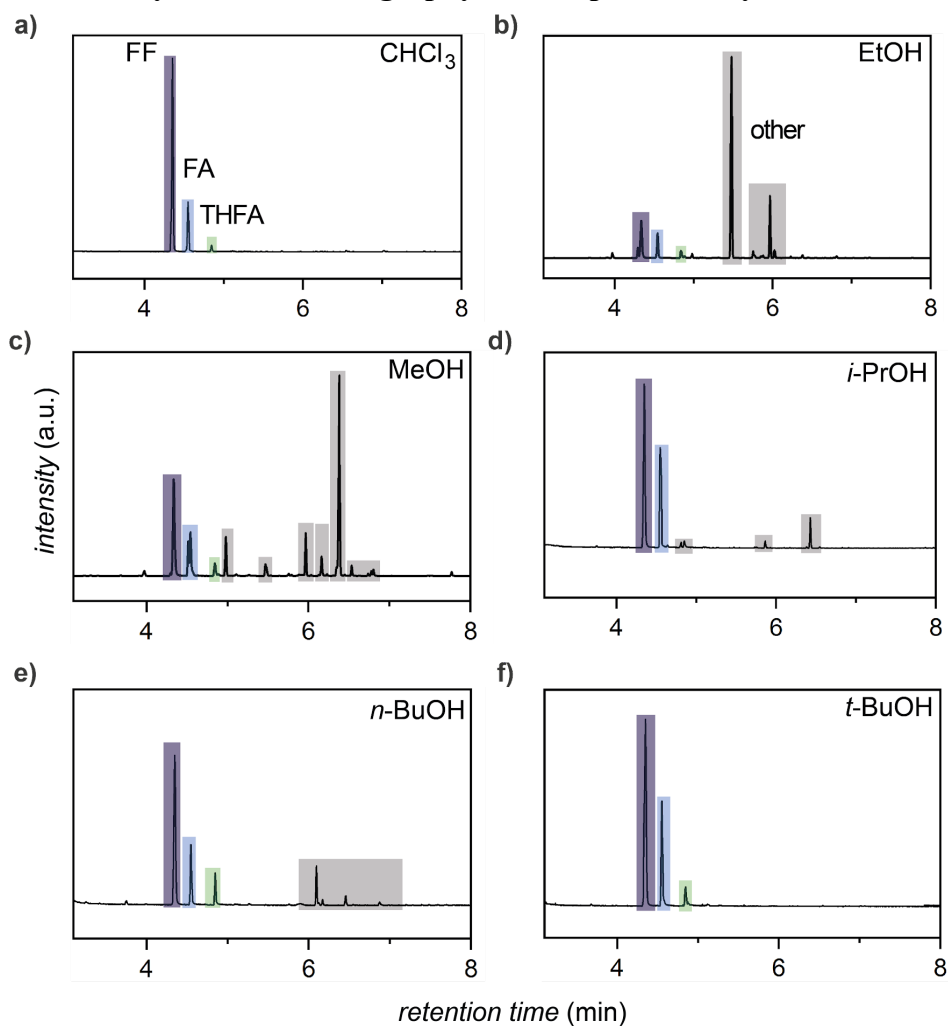


Figure S8: GC–MS measurements of furfural hydrogenation dissolved in: (a) CHCl₃; (b) EtOH; (c) MeOH (d) *i*-PrOH; (e) *n*-BuOH; and (f) *t*-BuOH. Furfural (FF; purple) is hydrogenated to form furfuryl alcohol (FA; blue), tetrahydrofurfuryl alcohol (THFA; green), and other side products (gray). These experiments were performed in MultiThor at 150 mA applied current and Pd/Pd membrane after 2 h of reaction.

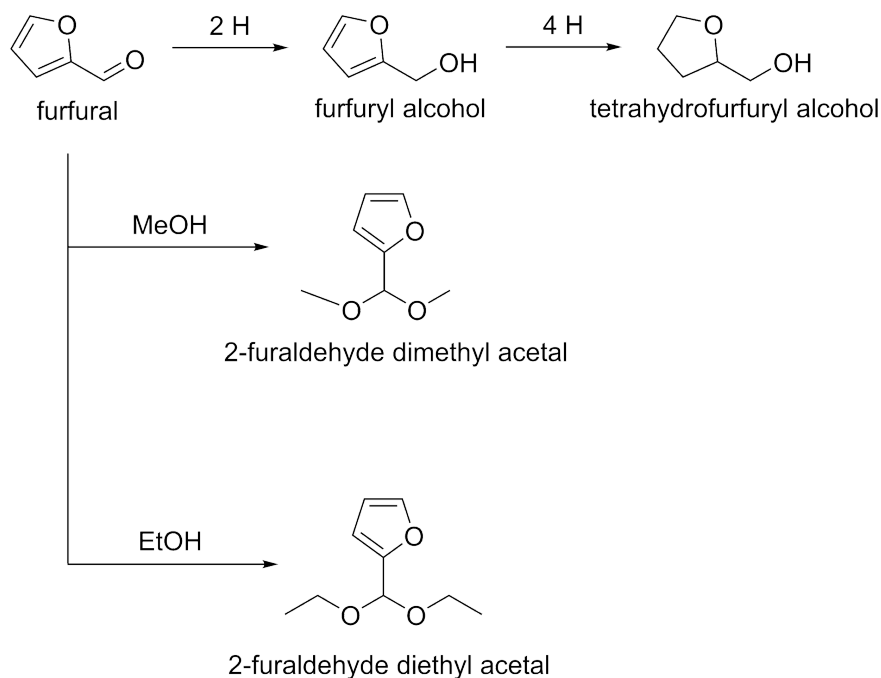


Figure S9: Furfural reaction pathway in the electrocatalytic palladium membrane reactor showing the acetal products formed when MeOH and EtOH are used as the solvent.

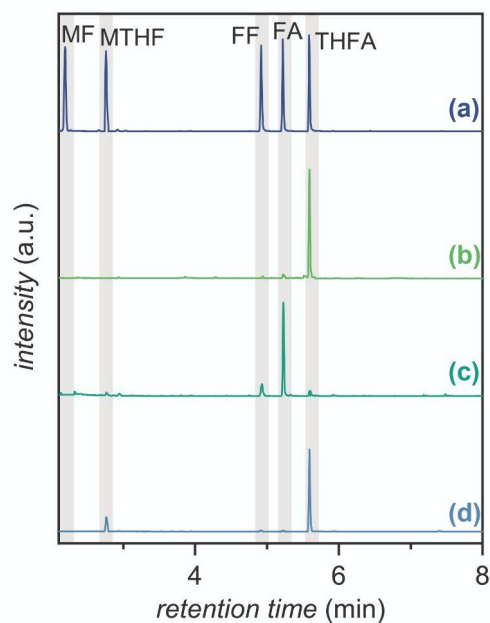


Figure S10. (a) GC–MS of standard solution containing 2-methylfuran (MF), 2-methyltetrahydrofuran (MTHF), furfural (FF), furfuryl alcohol (FA), and tetrahydrofurfuryl alcohol (THFA). (b) GC–MS of furfural hydrogenation with THFA selectivity at 225 mA using 10 nm Pt/Pd/Pd membrane after 8 h of reaction. (c) GC–MS of furfural hydrogenation with FA selectivity at 75 mA using 50 nm Pt/Pd/Pd membrane after 8 h of reaction. (d) GC–MS of furfural hydrogenation, where THFA hydrodeoxygenation leads to MTHF production at 225 mA using 10 nm Pt/Pd/Pd membrane after 24 h of reaction.

Influence of Current and Charge Passed on Furfural Hydrogenation Rates

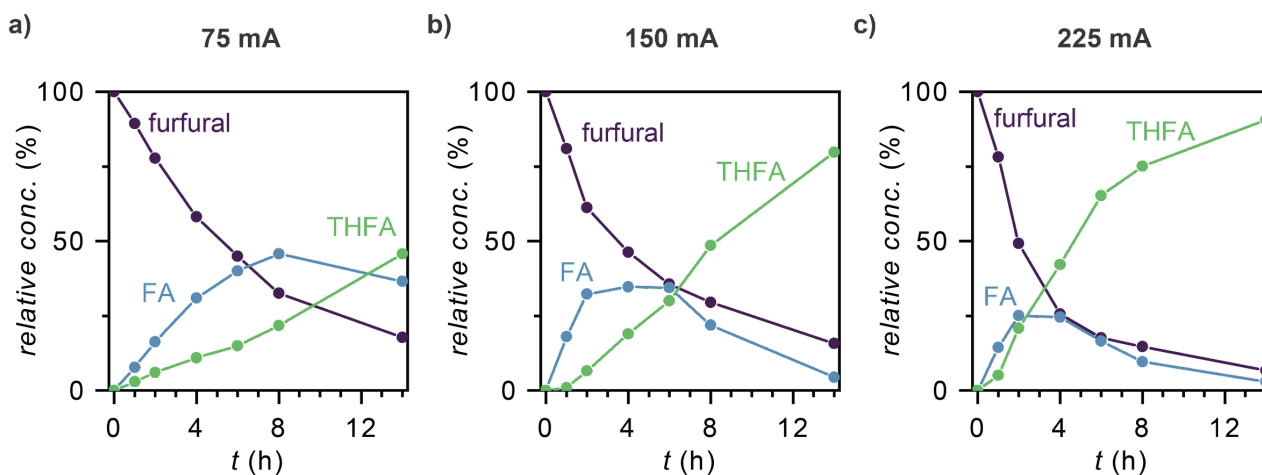


Figure S11. Plot of a reaction concentration profile for hydrogenation reaction of furfural to furfuryl alcohol (FA) and tetrahydrofurfuryl alcohol (THFA) carried out at: a) 75 mA; b) 150 mA; and c) 225 mA. The reaction was run with 0.25 M furfural in *t*-BuOH in the hydrogenation wells and a Pd/Pd membrane.

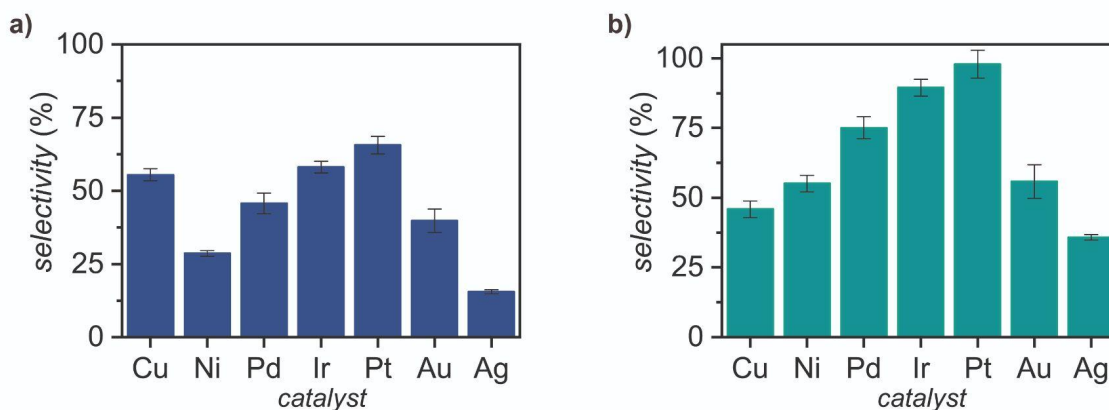


Figure S12. (a) Plot of selectivity for furfuryl alcohol (FA) at 75 mA after 8 h. (b) Plot of selectivity for tetrahydrofurfuryl alcohol (THFA) at 225 mA after 8 h of reaction. The reaction was run with 0.25 M furfural in *t*-BuOH in the hydrogenation wells. The error bars show triplicate experiments.

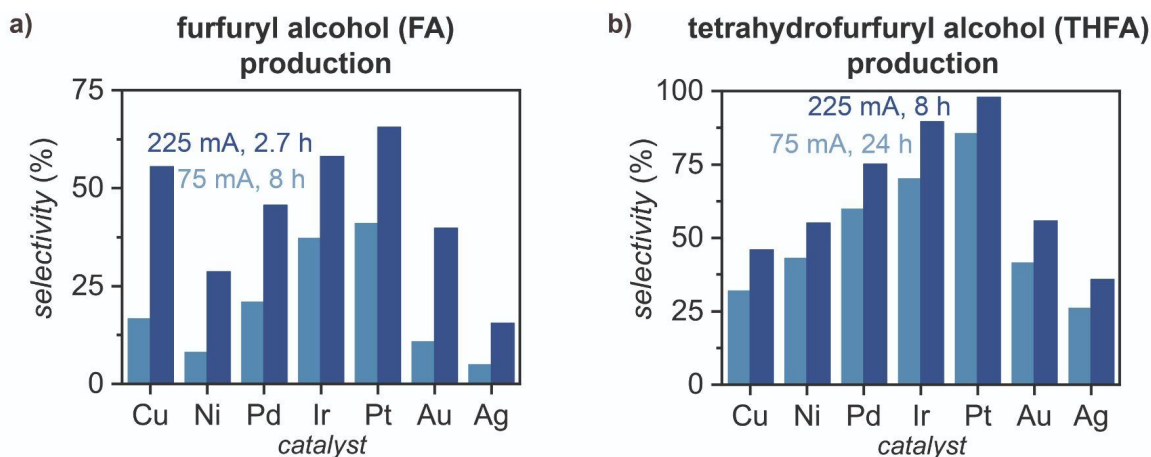


Figure S13. (a) Plot of selectivity for furfuryl alcohol (FA) at equivalent charge passed at 75 mA after 8 h and 225 mA after 2.7 h. (b) Plot of selectivity for tetrahydrofurfuryl alcohol (THFA) at equivalent charge passed at 75 mA after 24 h of reaction and 225 mA after 8 h of reaction. The observed trends suggest that charge passed is not the only factor that influences reactivity and selectivity. The reaction was run with 0.25 M furfural in *t*-BuOH in the hydrogenation wells and 10 nm of each sputter-deposited on a Pd/Pd membrane.

Influence of Sputter-Deposited Catalyst Thickness on Reactivity

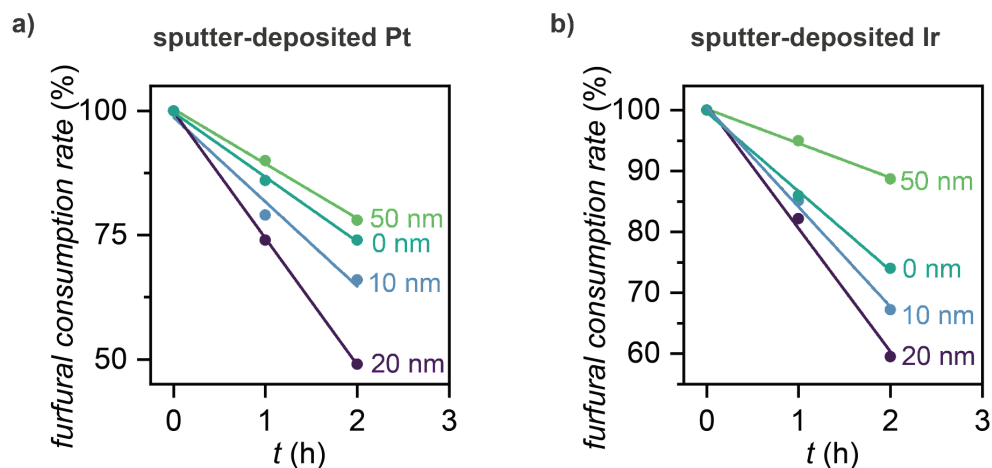


Figure S14: Initial consumption rate of furfural for different thicknesses (0, 10, 20, and 50 nm) of (a) Pt and (b) Ir sputter-deposited on a Pd/Pd membrane. The reaction was run at 75 mA with 0.25 M furfural in *t*-BuOH in the hydrogenation wells.

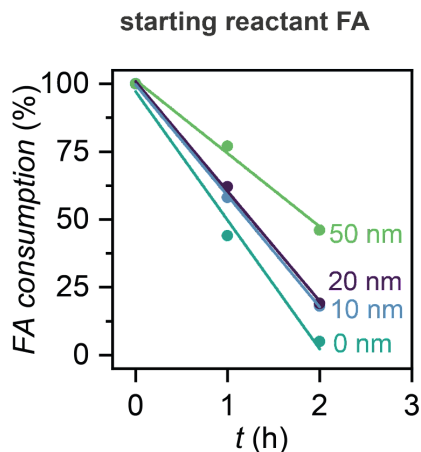


Figure S15: FA hydrogenation rates with 0, 10, 20, and 50 nm Pt/Pd/Pd membrane. The reaction was run at 75 mA applied current with 0.25 M furfural in *t*-BuOH in the hydrogenation wells.

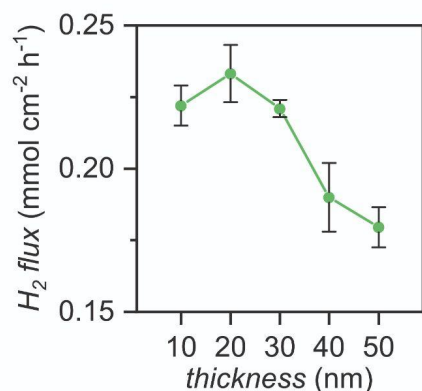


Figure S16: Hydrogen flux measurements for 10–50 nm of sputter deposited Ir on Pd/Pd membrane. The reaction was run at 75 mA with *t*-BuOH in the hydrogenation wells. H₂ flux was determined by atmospheric–mass spectrometer measurements of the ratio of evolved H₂ on the hydrogenation:electrochemical compartments.

Furfural Hydrogenation Without an Electrochemical Bias

A control experiment designed to study whether applying current directly to the palladium membrane affected hydrogenation rates was performed. A 75 mA current was applied across a Pt anode and secondary Pd cathode (i.e., not directly to the palladium membrane) in the MultiThor electrochemical reservoir called “without bias” in Fig. S17. The pump was set to a flow rate of 250 mL min⁻¹ for 1 h before current was applied to ensure the solution was saturated with H₂ gas. The

hydrogenation wells were filled with 0.25 M furfural in *t*-BuOH. The key difference between this configuration and our conventional ePMR setup was that H atoms produced from proton reduction would then form H₂ gas in the hydrogen evolution reaction. This H₂ gas could then: (i) spontaneously dissociate to form surface-adsorbed H atoms at the Pd membrane surface that then permeate through and participate in furfural hydrogenation; or (ii) bubble away in the form of H₂ gas in the electrochemical reservoir. Fig. S17 demonstrates that the conversion after 2 h of reaction with and without electrochemical bias was 36% and 6%, respectively. We ascribe this low conversion when a secondary Pd cathode is used to the fact that only a fraction of the hydrogen produced permeates the palladium membrane. Moreover, the use of coordinating electrolyte, H₂SO₄, has previously been shown to lead to low H₂ permeation across the palladium membrane in the ePMR, which may have also led to the low furfural consumption rates.² This low conversion highlights the importance of applying current directly to the palladium membrane.

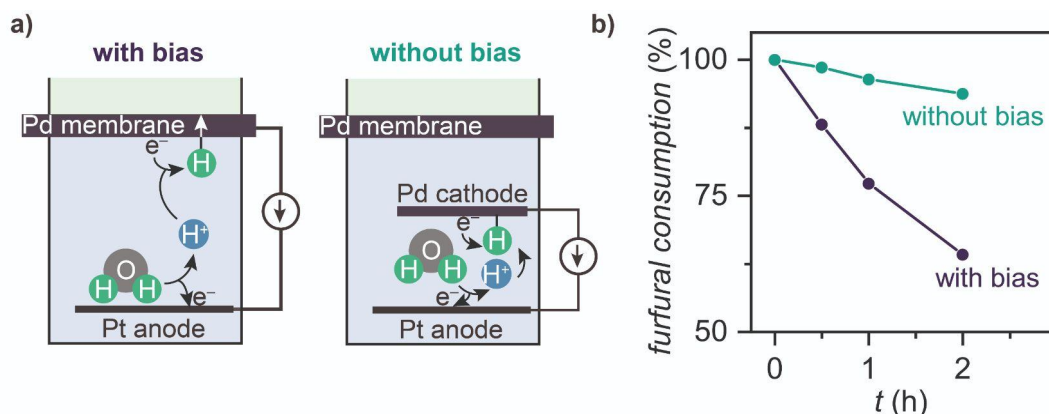


Figure S17: (a) Schematic diagram showing furfural hydrogenation with and without an electrochemical bias across the Pd membrane. (b) Furfural consumption over 2 h of reaction. For experiments with a bias, a 75 mA current was applied across a Pt anode and the Pd/Pd membrane in the electrochemical compartment. For experiments without a bias, a 75 mA current was applied across a Pt anode and a secondary Pd cathode placed in the electrochemical reservoir. Both reactions were run with 1 M H₂SO₄ in the electrochemical compartment and 0.25 M furfural in *t*-BuOH in the hydrogenation wells.

Supplementary References

- 1 A. Kurimoto, R. P. Jansonius, A. Huang, A. M. Marelli, D. J. Dvorak, C. Hunt and C. P. Berlinguette, *Angew. Chem. Int. Ed Engl.*, 2021, **60**, 11937–11942
- 2 R. S. Sherbo, R. S. Delima, V. A. Chiykowski, B. P. MacLeod and C. P. Berlinguette, *Nature Catalysis*, 2018, **1**, 501–507.
- 3 R. S. Delima, R. S. Sherbo, D. J. Dvorak, A. Kurimoto and C. P. Berlinguette, *J. Mater. Chem. A*, 2019, **7**, 26586–26595.
- 4 C. C. L. McCrory, S. Jung, J. C. Peters and T. F. Jaramillo, *J. Am. Chem. Soc.*, 2013, **135**, 16977–16987.
- 5 Y. Yoon, B. Yan and Y. Surendranath, *J. Am. Chem. Soc.*, 2018, **140**, 2397–2400.
- 6 A. Buttler and H. Spliethoff, *Renewable Sustainable Energy Rev.*, 2018, **82**, 2440–2454.